

RACS-SADL: Robust and Understandable Randomized Consensus in the Cloud

Pasindu Tennage
EPFL and ISTA
Lausanne, Switzerland
pasindu.tennage@epfl.ch

Antoine Desjardins
ISTA
Klosterneuburg, Austria
antoinedesjard@gmail.com

Lefteris Kokoris-Kogias
Mysten Labs and ISTA
Athens, Greece
lefteris@mystenlabs.com

Abstract—Widely deployed consensus protocols in the cloud are often leader-based and optimized for low latency under synchronous network conditions. However, cloud networks can experience disruptions such as network partitions, high-loss links, and configuration errors. These disruptions interfere with the operation of leader-based protocols, as their view change mechanisms interrupt the normal case replication and cause the system to stall.

We propose **RACS**, a novel randomized consensus protocol that ensures robustness against adversarial network conditions. **RACS** achieves optimal one-round trip latency under synchronous network conditions while remaining resilient to adversarial network conditions. **RACS** follows a simple design inspired by Raft, the most widely used consensus protocol in the cloud, and therefore enables seamless integration with the existing cloud software stack.

Experiments with a prototype running on Amazon EC2 show that **RACS** achieves 28k cmd/sec throughput, ninefold higher than Raft under adversarial cloud network conditions. Under synchronous network conditions, **RACS** matches the performance of Multi-Paxos and Raft, achieving a throughput of 200k cmd/sec with a median latency of 300ms, confirming that **RACS** introduces no unnecessary overhead. Finally, **SADL-RACS**, a throughput-optimized version of **RACS**, achieves a throughput of 500k cmd/sec, delivering 150% higher throughput than Raft.

Index Terms—consensus, adversarial, networks, scalability.

I. INTRODUCTION

Consensus [1] enables a set of replicas to maintain strongly consistent state while remaining resilient to failures, and is widely used in distributed cloud applications [2], [3], [4], [5], [6], [7], [8], [9], [10], [11], [12].

Most deployed consensus protocols in the cloud follow a leader-based design [3], [4], [13], [14]. The leader replica replicates client commands among the non-leader replicas and responds back to clients. Under normal case, where the network is synchronous, leader-based protocols provide moderate throughput and low latency.

Modern cloud networks [15], [16] use high-speed connections and are often synchronous. However, cloud networks can occasionally encounter adverse conditions such as high latency, packet loss, and partial connectivity [17]. These issues often stem from failing network hardware, congested links, inaccuracies in failure detection software, and flaws in monitoring systems [18], [19]. Hereafter, we refer to these

occasional adverse cloud network conditions as "adversarial network conditions".

In practice, leader-based protocols and their multi-leader extensions [20] [21] [22] [23] are designed to detect adversarial network conditions using timeouts [14]. If the leader replica does not respond within a pre-configured timeout, the remaining replicas elect a new leader replica. Electing a new leader replica often involves a separate "view change" sub routine [14], where each replica votes for a potential next leader replica.

View change-based leader election introduces performance and robustness challenges [24], [25]. During view change, no new client commands are committed, resulting in a prolonged commit delay for commands submitted during this period. Client commands proposed during the view change accumulate into a substantial backlog, causing significant overhead that persists even after the completion of the view change-based leader election. Since each replica buffers client commands during the view change, a significant backlog of commands accumulates by the time the leader election is completed. The large backlog of buffered commands places significant strain on the next elected leader, leading to further performance degradation.

Asynchronous consensus protocols [26] [27] ensure high robustness and performance under adversarial network conditions by leveraging randomization instead of relying on view change. However, to the best of our knowledge, asynchronous consensus protocols have never been deployed in cloud applications due to three main drawbacks: (1) they require significantly higher bandwidth compared to leader-based protocols [26]; (2) their design is often incompatible with the existing cloud software stack, hindering seamless integration and rapid adoption; and (3) their complexity makes them difficult to understand and implement, which limits industry adoption. Hence, cloud providers continue to deploy leader-based consensus protocols despite their limited robustness against adversarial network conditions [2].

Problem Statement: Can we design a consensus protocol that (1) remains robust under adversarial network conditions, (2) achieves performance comparable to leader-based protocols under synchronous network conditions, and (3) maintains a simple design that allows easy integration with the existing cloud software stack?

This paper proposes **RACS**, a robust and easily understandable randomized consensus protocol that addresses the above problem. **RACS** achieves three key goals:

- **G1:** Provides robustness against adversarial networks.
- **G2:** Matches the performance of high speed leader-based protocols [13], [14] under synchronous network conditions.
- **G3:** Employs an easy-to-understand design that seamlessly integrates with existing cloud software stack, enabling rapid adoption in the cloud.

Achieving robustness against adversarial network conditions has already been explored [25]–[28], and we explicitly state that this is “not” our primary contribution. Instead, **RACS**, our novel protocol, “simultaneously” achieves the three goals G1, G2, and G3—an accomplishment that no existing asynchronous protocol has achieved before. Designing **RACS** while achieving G1, G2 and G3 simultaneously is not trivial. First, designing a protocol that ensures robustness against adversarial network conditions without incurring additional overhead under synchronous conditions is a non-trivial algorithmic challenge. Second, designing a robust protocol while ensuring ease of understanding and compatibility with existing cloud software stacks is a challenge that no previous asynchronous consensus protocol has successfully addressed.

We implemented and evaluated **RACS** in Go [29] and compared it against the existing implementations of Multi-Paxos [13], Raft [14], and EPaxos [20]. We evaluated **RACS** on Amazon EC2 in a multi-region WAN setting. First, we show that **RACS** provides 28k cmd/sec of throughput, under adversarial network conditions, and outperforms Multi-Paxos and Raft which only provide 2.8k cmd/sec in the same setting. Second, we show that **RACS** delivers 200k cmd/sec in throughput under 300ms median latency, comparable to Multi-Paxos’s 200k cmd/sec throughput, under synchronous normal case conditions. Finally, we introduce novel optimizations for **RACS** and demonstrate that the optimized version; **SADL-RACS** achieves an impressive throughput of 500k cmd/sec.

A. Contributions

- We propose **RACS**, the first practical randomized consensus protocol that simultaneously achieves (1) robustness against adversarial network conditions, (2) high performance under typical synchronous network conditions, and (3) seamless integration with existing cloud software stack.
- We provide the formal proofs of **RACS** in Appendix A.
- We propose **SADL**, an optimization for **RACS** that enables high throughput and high robustness.
- We implement a prototype of **RACS** and conduct an experimental analysis on Amazon EC2.
- We show that **RACS** achieves nine times greater robustness than Raft under adversarial network conditions, while **SADL-RACS** delivers 150% higher throughput than Raft.

II. BACKGROUND AND RELATED WORK

A. Threat Model and Assumptions

We consider a system with n replicas. Up to f (where $n=2f+1$) number of replicas can crash, but replicas do not

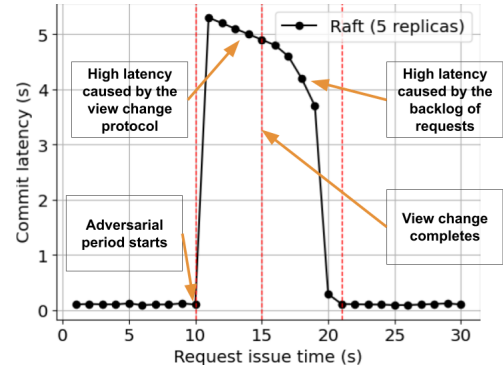


Fig. 1: High latency overhead due to view change in Raft.

equivocate nor commit omission faults [1].

We assume first-in-first-out (FIFO) perfect point-to-point links [1] between each pair of replicas. In practice, TCP [30] provides FIFO perfect point-to-point links. We assume a content-oblivious [31] network adversary; the adversary may manipulate network delays, but cannot observe the message content nor the internal replica state. In practice, TLS [32] encrypted channels between each pair of replica satisfy this assumption.

FLP [33] impossibility result claims that no deterministic protocol can guarantee both safety and liveness in a fully asynchronous system with even one faulty process. Practical protocols address the FLP [33] impossibility using two approaches: (1) assuming partial synchrony, and (2) using randomization. Protocols like Raft [14] and Multi-Paxos [13] assume partial synchrony and ensure safety at all times, however, lose liveness under asynchrony. Randomized protocols, in contrast, employ randomness instead of determinism, preserving safety always and ensuring liveness under asynchrony with probability 1.

In a typical cloud network, there are periods in which the network behaves synchronously, followed by phases where the network shows adversarial behavior. **RACS** makes use of this network behavior and operates in two modes: (1) synchronous mode and (2) fallback mode. During the synchronous periods, **RACS** employs a leader-based design to reach consensus using one round trip network delay, and during the fallback mode, **RACS** employs randomization.

B. Consensus

Consensus enables a set of replicas to reach an agreement on a single history of values. A correct consensus algorithm satisfies four properties [1]: (1) *validity*: the agreed upon value should be previously proposed by a replica, (2) *termination*: every correct process eventually decides some value, (3) *integrity*: no process decides twice, and (4) *agreement*: no two correct processes decide differently.

Robustness problem in leader-based protocols: Multi-Paxos [13], Raft [14], and View Stamp Replication [34] employ a single leader replica to totally order commands. Under normal network conditions, the leader replica replicates client commands in one network round trip. When the network conditions become adversarial, leader-based protocols run a separate “view-change” sub-routine that elects a new

leader replica. View change introduces robustness challenges in leader-based protocols, which we illustrate using Figure 1.

In Figure 1, we run Raft—the most widely deployed consensus protocol in the cloud—with 5 replicas, with the view timeout configured at 5 seconds. At time $t = 10s$ seconds, we simulate an adversarial network condition by introducing a 6-second delay on the links connected to the current leader. We first observe that the commands issued between 10s and 15s experience significantly high commit latency. This high latency arises from the view change, as no new commands are committed until the view change is fully completed. Second, we observe that commands issued after the completion of the view change also experience high commit latency. This is due to the backlog of commands that accumulated during the view change. Therefore, existing leader-based consensus protocols are unable to ensure robustness under adversarial network conditions. In contrast, RACS, our novel protocol, ensures robustness under adversarial network conditions.

Multi-leader protocols [20], [21], [23], [24] and other extensions of leader-based protocols [35] [36] [22] [37] also lose liveness under adversarial network conditions due to their reliance on view change mechanisms.

Randomized consensus protocols [27] [26] overcome the adversarial network challenge by using randomization instead of view changes. However, they are rarely used in cloud applications due to (1) high performance overhead under synchronous network conditions, (2) incompatibility with the existing cloud software stack, and (3) complexity in understanding and implementing. In contrast, our protocol RACS provides a practical solution to adversarial network challenges by achieving: (1) robustness under adversarial network conditions, (2) optimal one round-trip commit latency under synchronous networks, and (3) a simple design for fast implementation and seamless industry adoption.

Rabia [38] and RACS take opposite paths on the simplicity–robustness tradeoff. Rabia [38] aims for simplicity in synchronous LANs but loses liveness under WAN asynchrony. In contrast, RACS ensures liveness under asynchrony. Rabia’s [38] leaderless design differs from Paxos/Raft standard leader-based model, requiring ground-up changes in the implementation, making adoption costly. Rabia [38] has quadratic message complexity, whereas RACS has linear message complexity, under synchrony.

QuePaxa [25] solves the asynchronous consensus challenge, however, significantly differs from RACS in design. QuePaxa [25] uses randomized local-coins and splits the replica role into separate proposer role and recorder role. In contrast, RACS employs global-coins and closely follows the standard Raft model.

Mahi-Mahi [39], Tusk [28], and Dag-Rider [40] are “blockchain” asynchronous protocols targeting Byzantine faults, which is out of our scope. We omit detailed comparisons due to space and relevance.

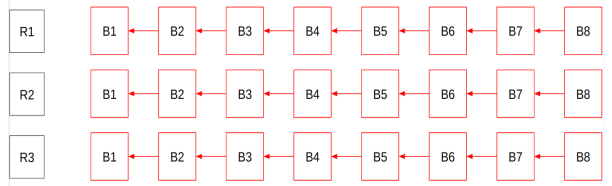


Fig. 2: Replicated log of RACS replicas.

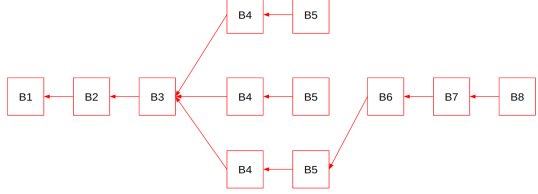


Fig. 3: Fallback mode of RACS.

III. RACS

A. RACS Protocol Overview

We introduce RACS, a novel crash fault-tolerant randomized consensus algorithm. RACS achieves three important goals: (1) robustness against adversarial network conditions, (2) performance comparable to existing leader-based protocols under synchronous network conditions, and (3) simplicity in design, enabling rapid implementation and seamless integration into existing cloud software stack.

Given the wide adoption of Raft [14] in cloud software [41], [42], we design RACS by extending Raft. Building RACS on Raft as the foundation facilitates its rapid adoption in cloud environments, because existing cloud software stacks already support the programming abstractions and infrastructure required by Raft.

As illustrated in Figure 2, similar to Raft [14], each replica in RACS maintains a sequential log of blocks. Each block points to the previous block using a pointer. The purpose of RACS protocol is to ensure that each replica commits the same value for each block, despite replica and network failures.

Similar to Raft, RACS employs a leader-based design during the synchronous network conditions. The leader replica in RACS collects a batch of client commands, and replicates them in at least a majority of the replicas. Replication under synchronous network conditions takes one network round trip, the theoretical optimal. As long as the network conditions remain synchronous and the leader replica doesn’t crash, RACS commits commands in one network round trip.

Under adversarial network conditions, Raft employs a view change sub-routine, where each replica votes for a potential new leader replica. As shown in Figure 1, view change based leader election harms the performance. In RACS, we eliminate view change-based leader election, marking a fundamental difference from Raft. Instead of view-change based leader election, RACS employs a novel randomized fallback mode that keeps committing new client commands. Replacing view change sub routine with the randomized fallback mode of operation is the key difference between Raft and RACS.

Figure 3 illustrates the randomized fallback mode of **RACS** from the perspective of a single replica. In Figure 3, the network remains synchronous until block B3 is replicated. Due to an adversarial network condition, the leader replica fails to transmit B4, and therefore all the replicas “automatically” enter the randomized fallback mode of operation. During the randomized fallback mode, each replica, independent from other replicas, act as a leader, and proposes new blocks. As shown in Figure 3, in a 3 replica configuration, the randomized fallback mode results in 3 parallel chains of blocks. The number of blocks proposed during the randomized fallback mode can be configured dynamically, but for the purpose of illustration, in this example we use two fallback blocks. Once each replica has proposed 2 fallback blocks, they consistently chose a single chain (the last fallback chain in Figure 3) out of all available fallback chains. If adversarial conditions persist, another round of fallback mode will be triggered. Otherwise, the synchronous path leader of the next view will replicate blocks in a single network round trip, extending the chosen fallback chain.

Replacing view change in Raft with a randomized fallback mode helps **RACS** achieve the three goals mentioned above. First, because new commands are committed in the randomized fallback mode, **RACS** remains robust under adversarial network conditions. Second, during the synchronous periods of execution, **RACS** uses a leader-based design, and incurs the same overhead as Raft. Finally, because **RACS** builds on Raft, it is easy to understand and requires fewer additions to the existing Raft implementations [42], [43], enabling rapid adoption in the cloud. **RACS** is the first protocol to simultaneously achieve all 3 goals.

B. RACS Algorithmic Challenges

RACS has a simple design but faces non-trivial challenges in ensuring agreement and termination. First, depending on the network conditions, **RACS** must automatically switch between the synchronous single-chain mode and the fallback multi-chain mode, without manual intervention. Second, **RACS** must ensure that each replica commits the same chain of blocks, even when multiple chains exist during adversarial periods – each replica should consistently choose the same fallback chain at the end of the fallback mode. Section III-C addresses these challenges and presents the **RACS** algorithm.

C. RACS Algorithm

Similar to Raft, **RACS** progresses as a sequence of **views** v and **rounds** r where each view has one or more rounds. A view consists of (1) a synchronous mode with a predefined leader $L_{v_{cur}}$ and (2) a fallback mode of operation. In Figure 3 blocks B1–B5 are from the same view, where blocks B1–B3 are synchronous mode blocks and blocks B4–B5 are fallback mode blocks. Blocks B6–B8 are from the next view. A round represents the successive log positions in the replicated log. Round numbers are monotonically increasing. The pair (v, r) is called a **rank**.

Block Format: There are two types of **RACS** blocks: (1)

synchronous blocks and (2) **fallback blocks**. Both types of blocks consist of five fields: (1) batch of client commands, (2) view number, (3) round number, (4) parent block, and (5) level. The rank of a block is (v, r) and blocks are compared lexicographically by their rank: first by the view number, then by the round number. The blocks are connected in a chain using the parent links. We denote that block A **extends** block B if there exists a set of blocks $b_1, b_2, b_3, \dots, b_k$ such that there exists a parent link from b_i to $b_{i-1} \forall i \in \text{range}(2, k)$ and $b_1 = B$ and $b_k = A$. The level field of the block refers to the fallback level. For the synchronous blocks, the level is always set to 0.

Fig. 4 depicts the pseudo-code of **RACS**. In the following discussion, when we say replica p_i delivers a block B from replica p_j , we imply that replica p_i delivers B and the causal history of B .

Synchronous mode: The synchronous mode of **RACS** is leader-based and is similar to Raft, as depicted in lines 1–11 of Figure 4.. The synchronous mode leader $L_{v_{cur}}$ for each view v is predetermined and known to all replicas on bootstrap, for example $L_{v_{cur}} = v_{cur} \% n$. As we discuss below, $L_{v_{cur}}$ begins its tenure only after receiving a quorum of $\langle \text{vote} \rangle$ messages, which allows $L_{v_{cur}}$ to learn the most up-to-date block—a condition indirectly achieved in Raft [14] by electing the most up-to-date replica during view change.

The synchronous mode begins either at the very start of the protocol or after a fallback mode has ended. Upon collecting a $n/2 + 1$ number of $\langle \text{vote} \rangle$ messages, the leader replica forms a new block B , that extends the $block_{high}$ (see line 3 of Figure 4). The leader then broadcasts a $\langle \text{propose} \rangle$ message for the block B and the reference of the last committed block $block_{commit}$ (see line 4 of Figure 4).

Each replica p_i delivers $\langle \text{propose}, B, block_c \rangle$ message, if the rank of B is greater than the rank of p_i and if p_i is in the synchronous mode of operation. If these two conditions are met, then p_i first updates its $block_{high}$, v_{cur} , r_{cur} (see line 6–7 of Figure 4) and then commits the block $block_c$ (see line 8 of Figure 4). p_i then sends p_i ’s $\langle \text{vote} \rangle$ for B to $L_{v_{cur}}$ (see line 9 of Figure 4).

Upon receiving $n/2 + 1$ $\langle \text{vote} \rangle$ messages for B (see line 1 of Figure 4), the leader replica commits B (and the causal history). As long as the synchronous mode leader $L_{v_{cur}}$ is responsive, the synchronous mode will continue, committing a new block in one network round trip.

Each replica has a timeout clock which is reset whenever the replica receives a new $\langle \text{propose} \rangle$ message (see line 5 of Figure 4). If the timeout expires (see line 11 of Figure 4), however, they will broadcast a $\langle \text{timeout} \rangle$ message containing the $block_{high}$.

Fallback mode: The number of blocks proposed during the fallback mode is a tunable parameter that we explain in Section IV-A. For simplicity of illustration, we use 2 fallback blocks per view in the following description. Upon receiving $n/2 + 1$ $\langle \text{timeout} \rangle$ messages, **RACS** enters the fallback mode of operation. In the fallback mode, all replicas act as leaders. Each replica takes the highest $block_{high}$ they

RACS Protocol for replica p_i , $i \in 0..n-1$

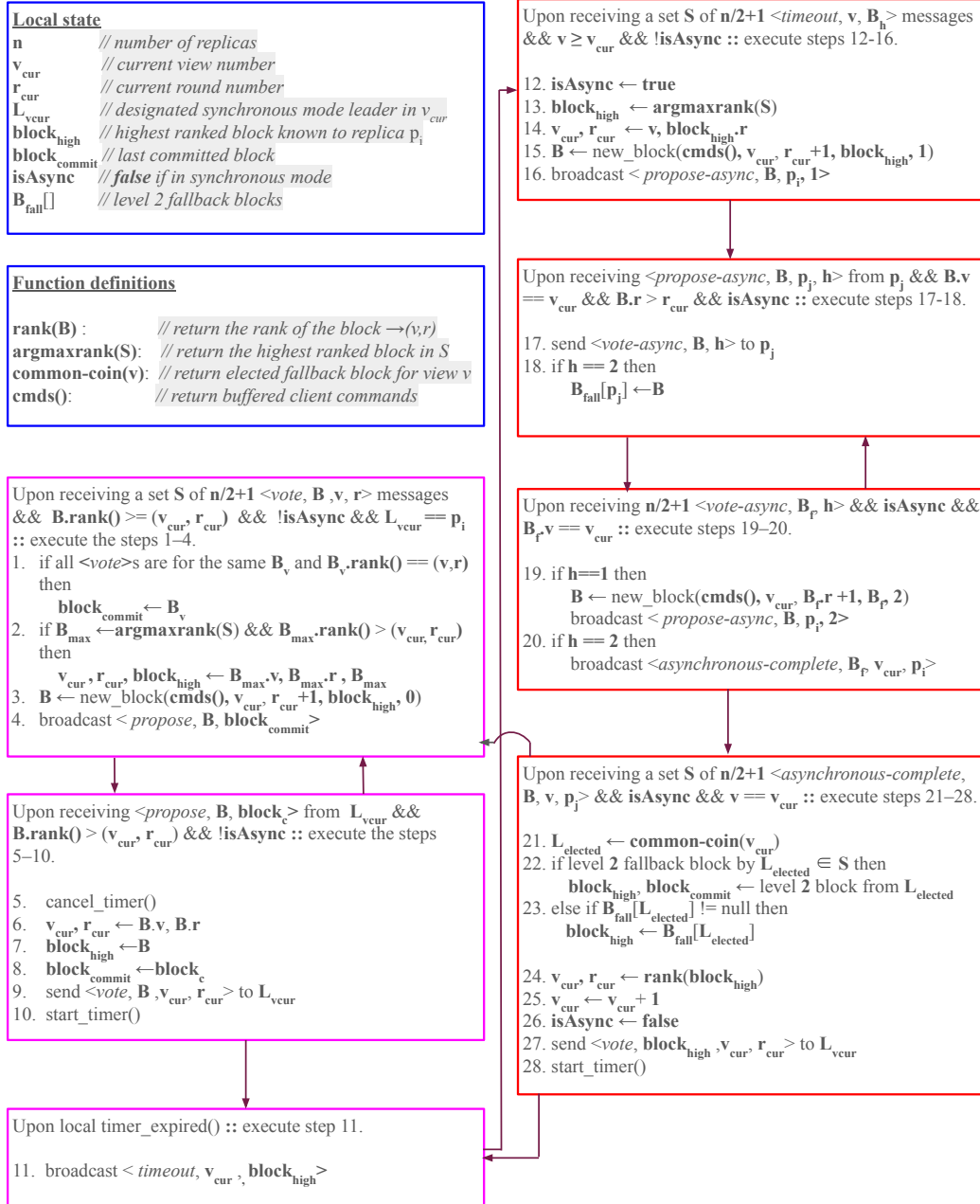


Fig. 4: RACS Algorithm.

are aware of, forms a level 1 fallback block B with a monotonically increasing rank compared to the highest $block_{high}$ it received and sends a $<propose-async>$ message (see line 12-16 of Figure 4).

Upon receiving a $<propose-async>$ message from p_j , each replica p_i sends back a $<vote-async>$ message to p_j if the rank of the proposed level 1 block is greater than the highest-ranked block witnessed so far (see line 17 of Figure 4).

Upon receiving $n/2 + 1$ $<vote-async>$ messages for the level 1 fallback block B_f , each replica will send a level 2

fallback block B (see line 19 of Figure 4). The algorithm allows catching up to a higher ranked block by building upon another replica's level 1 block. This is meant to ensure termination for replicas that fall behind. All replicas, upon receiving a $<propose-async>$ message for a level 2 fallback block from p_j send a $<vote-async>$ message to p_j (see line 17-18 of Figure 4).

Once $n/2 + 1$ $<vote-async>$ s have been gathered for the level 2 fallback block B_f , each replica p_i broadcasts an $<asynchronous-complete>$ message (see line 20 of Figure 4).

Once $n/2 + 1$ replicas have submitted $\langle \text{asynchronous-complete} \rangle$ messages, the fallback mode is complete. The remaining task is to consistently select one chain from the set of fallback chains. This step is crucial for maintaining agreement. If two replicas select different fallback chains, the system loses the guarantee that all replicas commit the same sequence of blocks. To ensure that each replica consistently chooses the same chain, we employ a **common-coin**, an existing technique [26], [38] used in distributed algorithms.

Common-coin: For each view v , $\text{common-coin}(v)$ returns a positive integer in the range $(0, n - 1)$ where n is the total number of replicas. The invocation of $\text{common-coin}(v)$ for a given view v , at each replica returns the same value.

RACS uses a common-coin mechanism, where each replica runs a consistent random number generator with a pre-agreed seed. When used with the same seed, consistent random number generation protocols produce the same output sequence. Common-coin enables **RACS** to consistently choose a fallback chain after completing fallback mode.

Upon receiving $n/2 + 1$ $\langle \text{asynchronous-complete} \rangle$ messages, each replica individually flips a common-coin (see line 21 of Figure 4) to get the elected leader L_{elected} . Each replica commits a level 2 fallback block B from L_{elected} if B arrived amongst the first $n/2 + 1$ $\langle \text{asynchronous-complete} \rangle$ messages (see line 22 of Figure 4). If a replica observes that the level 2 fallback block from L_{elected} does not appear in the first $n/2 + 1$ $\langle \text{asynchronous-complete} \rangle$ messages, but appears in $B_{\text{fall}}[L_{\text{elected}}]$, then, the replica sets $\text{block}_{\text{high}}$ to $B_{\text{fall}}[L_{\text{elected}}]$ (see line 23 of Figure 4). All replicas then exit the fallback mode and resume the synchronous path by unicasting a $\langle \text{vote} \rangle$ message to the synchronous leader L_{vcur} of the next view (see line 27 of Figure 4).

RACS fallback mode ensures liveness under adversarial network conditions; it only requires receiving at least $n/2 + 1$ messages in each asynchronous step. This quorum condition is trivially satisfied under the standard assumption that fewer than $n/2$ nodes can fail and with reliable point-to-point links (TCP). Thus, delayed messages or timeout settings do not impact the asynchronous liveness guarantee of **RACS**.

RACS protocol summary: Based on the above **RACS** explanation, its outcomes are summarized as follows. **RACS** ensures robustness against adversarial network conditions by committing new commands during the randomized fallback mode. **RACS** commits client commands in one network round trip, and hence provides optimal synchronous normal case latency. Finally, because **RACS** follows a simple design and extends Raft, it enables seamless integration with the existing cloud software stack. Although the **RACS** fallback mode modifies Raft [14] in non-trivial ways, the fallback mode employs the same replica and network structures, without requiring any additional cloud software stack changes. Thus, **RACS** remains fully compatible with existing cloud software stack and requires only incremental integration effort.

D. Correctness and Complexity

The formal proofs have been deferred Appendix A.

Agreement property: **RACS** satisfies the agreement property by ensuring that if a block B is committed in any round r , then all the blocks with round $r' \geq r$ will extend B .

Termination property: **RACS** ensures termination under both synchronous and adversarial network conditions, due to common-coin based randomization.

Complexity The synchronous mode of **RACS** has a linear message and bit complexity for committing a block. The fallback mode of **RACS** has a complexity of $O(n^2)$.

IV. RACS OPTIMIZATIONS

A. Tuning fallback blocks

In Section III, we described **RACS** with two fallback blocks per view. In practice, fixed blocks per view are suboptimal under unpredictable adversarial conditions.

In **RACS**, we dynamically adjust the number of blocks in fallback mode using Multi-Armed Bandit techniques [44]. We bootstrap **RACS** with 2 blocks per fallback mode, and each replica monitors s : the number of times the algorithm switches between synchronous and fallback mode. A high s implies a network where adversarial conditions persist, whereas a low s indicates a transient network problem. **RACS** employs a Multi-Armed Bandit-based explore/exploit strategy, increasing the number of blocks per fallback mode when s increases and decreasing it when s decreases. **RACS** uses the same technique as Raft's reconfiguration to consistently configure s across all replicas. Further details are omitted due to space.

B. Application specific optimizations

Cloud applications that employ consensus protocols can be broadly categorized into two groups based on their performance objectives: (1) **Class 1**: applications that require moderate throughput and low latency [2] [45] [3] and (2) **Class 2**: applications that require high throughput and can tolerate moderately high latency [46] [47].

For class 1 applications, we employ *pipelining*, a well-established technique in distributed algorithms [13], [25]. In pipelined-**RACS**, the synchronous mode leader L_{vcur} proposes multiple blocks before receiving $n/2 + 1$ $\langle \text{vote} \rangle$ messages, allowing multiple blocks to be committed within a single round-trip network latency.

1) Optimization for class 2 applications

RACS blocks contain two types of data: (1) metadata about the block such as v , and r , and (2) a batch of client commands. Typically, the metadata is only a few bytes in size, while the batch of client commands can span several kilobytes. Bundling both metadata and client commands within **RACS** blocks increases the block size, which limits the system's throughput due to the bandwidth bottleneck at the leader replica. This is a significant limitation of **RACS**, particularly for class 2 applications that demand high throughput.

To address this limitation, we propose **SADL**, a novel command dissemination layer that decouples command dissemination from the critical path of the consensus protocol. **SADL** is a consensus-agnostic command dissemination layer

SADL Protocol for replica p_i , $i \in 0..n-1$	
<u>Local state</u>	
tips[]	// last confirmed SADL-batch rounds
chains[][]	// k^{th} SADL-batch from replica p_j
buffer	// pending client commands
awaiting \leftarrow false	
batch time	
batch size	
<u>Function definitions</u>	
cmds()	// returns tips
Upon size of buffer reaching batch size or the batch time is reached and !awaiting :: execute steps 1–4.	
1. $B_{\text{parent}} \leftarrow \text{chains}[p_i][\text{tips}[p_i]]$	
2. $B \leftarrow (\text{tips}[p_i]+1, B_{\text{parent}}, \text{buffer.popAll}())$	
3. awaiting \leftarrow true	
4. broadcast $\langle \text{SADL-Batch}, B \rangle$	
Upon receiving $\langle \text{SADL-Batch}, B \rangle$ from p_j :: execute steps 5–7.	
5. $\text{chains}[p_j][B.r] \leftarrow B$	
6. $\text{tips}[p_j] \leftarrow B.\text{parent.r}$	
7. send $\langle \text{SADL-vote}, B.r \rangle$ to p_j	
Upon receiving $n/2 + 1 \langle \text{SADL-vote}, r \rangle$ and $r = \text{tips}[p_i]+1$ and awaiting :: execute steps 8–9	
8. awaiting \leftarrow false	
9. $\text{tips}[p_i] += 1$	

Fig. 5: SADL Algorithm.

designed to reliably distribute client commands to at least a majority of replicas, ensuring efficient and fault-tolerant command propagation. SADL provides fault tolerance and availability for individual client batches, but does not guarantee a total order of commands. Once SADL replicates commands across a majority of replicas, RACS layer no longer needs to include the commands in its blocks. Instead, RACS only embeds a small, fixed-size “reference” to the batch already disseminated by SADL. Using a fixed-size reference instead of the entire command batch significantly reduces the RACS leader replica’s bandwidth consumption, leading to a substantial improvement in throughput, as demonstrated in Section VI.

SADL design significantly differs from existing dissemination approaches. Unlike existing dissemination mechanisms [28], [48], where the dissemination layer advances in a lock-step fashion, SADL allows each replica to build its own chain of SADL blocks independently of the pace of other replicas. This key difference enables SADL to achieve higher throughput than existing approaches. We present this subtle yet non-trivial distinction as a novel systems contribution of this paper.

SADL Protocol: Figure 5 depicts the SADL pseudo code. In SADL, each replica concurrently proposes SADL batches. For clarity of presentation, we describe the algorithm from the perspective of a single replica p_i . Upon receiving a batch of commands, replica p_i creates a new SADL batch B , extending its last created SADL batch B_{parent} , and broadcasts a $\langle \text{SADL-Batch}, B \rangle$ message (see lines 1–4 of Figure 5). Other replicas, upon receiving a new $\langle \text{SADL-Batch}, B \rangle$, store

B in **chains**, update **tips** to the round number of the parent of B , and send a $\langle \text{SADL-vote} \rangle$ to p_i (see lines 5–7 of Figure 5). Replica p_i , upon receiving $n/2 + 1 \langle \text{SADL-vote} \rangle$ messages for its last proposed block B , updates the **tips** (see line 9 of Figure 5) and starts proposing a new SADL-batch (see lines 1–4 of Figure 5).

Replica p_i broadcasts the next SADL batch only after receiving $n/2 + 1$ votes for the previous SADL batch it proposed. Hence, any replica, upon receiving a new SADL batch B from p_i , can be certain that all SADL batches from p_i , prior to B have already been replicated in at least a majority of the replicas. This property of SADL enables it to reference a large batch of client commands using a fixed-size integer array of several bytes. The **tips** integer array of size **n** stores the last successfully committed SADL batch for each replica, thereby allowing the entire set of client batches to be represented using a fixed-size integer array.

Using SADL with RACS: With SADL in place, RACS blocks no longer need to carry the heavy client batches and instead include only the **tips** integer array as the proposal for consensus. Upon committing a block in RACS, RACS commits all uncommitted batches in all SADL chains up to the last block pointed to by the **tips** array, effectively committing a consistent cut of the SADL chains. Since **tips** is an array of **n** elements, the size of RACS blocks is drastically reduced, effectively eliminating the leader bottleneck problem in the RACS synchronous mode. As we show in Section VI, SADL significantly increases throughput, albeit with a modest increase in latency. Therefore, for class 2 applications that require high throughput but can tolerate moderately high latency, SADL is well-suited.

V. IMPLEMENTATION

We implemented pipelined-RACS and SADL-RACS using Go version 1.19 [29], in 3661 and 4631 lines of codes, respectively. We used the standard Go network library and Protobuf encoding [49]. We used a single-threaded event based design for RACS’s main event handling logic. All events—message receipt, timeouts, etc.—are handled by a single thread, ensuring deterministic event execution. For better I/O performance, we use multiple threads for TCP message reception, as done in prior work [25], [38], [43]. Both RACS and SADL-RACS implement batching in both clients and replicas. SADL-RACS implementation is publicly available on github¹.

VI. EXPERIMENTAL EVALUATION

This evaluation demonstrates the following 4 claims.

- **C1:** RACS offers robustness against adversarial network conditions.
- **C2:** Under synchronous network conditions, RACS performs comparably to existing leader-based algorithms.
- **C3:** SADL-RACS delivers high throughput for class 2 applications that demand high throughput.
- **C4:** SADL improves the scalability of RACS w.r.t (C4.1) increasing replica count and (C4.2): increasing payload size.

¹<https://github.com/ISTA-SPiDerS/sadl-racs>

Since adversarial networks are much more common in the wide-area network (WAN) than in the local-area network (LAN), we focus on the WAN deployments in our evaluation, however, for completeness of experiments, we also compared the performance of RACS in a LAN in Section VI-D.

We compare RACS’s and SADL-RACS’s performance against three state-of-the-art SMR algorithms: Raft [14] [43], Multi-Paxos [13] [43], and EPaxos [20] [50]. Raft and Multi-Paxos are the most widely used consensus algorithms in cloud environments. EPaxos is a multi-leader protocol that enables parallel commits of non-interfering commands.

Setup: We test both a WAN setup where the replicas and clients are distributed globally across AWS cloud regions Sydney, Tokyo, Seoul, Osaka, and Singapore and a LAN setup where all replicas and clients are located in North California AWS cloud.

For WAN experiments, we chose t2.xlarge EC2 instances [51] with 4 vCPUs and 16 GB memory. For LAN experiments, we use instances of type c4.4xlarge (16 virtual CPUs, 30 GB memory) for replicas and clients. Since CPU is often the bottleneck in LAN settings—where network latency is low and available bandwidth is high—it is standard to use machines with more CPUs for LAN experiments and we followed this established practice. To ensure a fair, apples-to-apples comparison, we ran Raft, Multi-Paxos, and EPaxos on the same testbed. We use Ubuntu Linux 20.04.5 LTS [52].

Workload and Benchmarks: Following the existing implementations Multi-Paxos and Raft [43], we use a *map[string]string* key-value store and Redis [53] as backend applications.

In our experiments, we use n replicas and n clients. Clients generate client commands with a Poisson distribution in the open-loop model [54]. All algorithms employ batching in both clients and replicas. A single client command is a 17 bytes string: 1-byte GET/PUT opcode plus 8-byte keys and values, consistent with command sizes used in prior research and production systems [11], [38].

As the initial leader replica of Multi-Paxos [13], Raft [14], and RACS, we selected the replica located in Tokyo AWS region. We tested with other initial leader replica locations (Sydney, Seoul, Osaka, and Singapore), however, observed no noticeable performance difference. In Multi-Paxos and Raft, once a view timeout occurs, the next leader is selected uniformly at random – whoever initiates and successfully completes the view-change sub-routine becomes the leader for the subsequent view. In RACS, we use a deterministic round-robin next leader scheme for each new view.

For RACS, SADL-RACS, Multi-Paxos, and Raft we measure the client observed end-to-end execution latency, which accounts for the latency overhead for total ordering and executing commands. EPaxos provides two modes of operations: (1) partial ordering of commands without execution (denoted “EPaxos-commit” in the graphs) and (2) partial ordering of commands with execution (denoted “EPaxos-exec” in the graphs). Trivially, “EPaxos-commit” outperforms RACS and SADL-RACS because “EPaxos-commit” only provides a

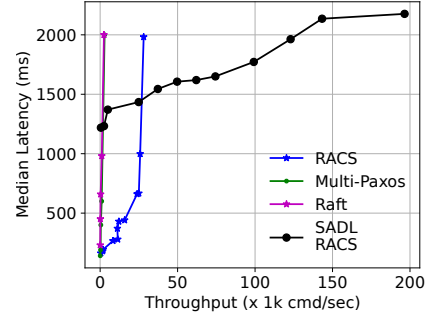


Fig. 6: Adversarial Performance in the WAN with 5 replicas.

partial order of commands, which enables higher parallelism. Hence, “EPaxos-commit” provides an apples-to-oranges comparison, however, we present the results in this evaluation, for completeness. We also found and reported bugs in the existing implementation of EPaxos code that prevent execution under adversarial network conditions, crashes, and when deployed with more than 5 replicas. Hence we use EPaxos only under normal-case performance evaluation.

We measure throughput in commands per second (cmd/sec), where a command is one 17-byte command. We measure the latency in milliseconds.

A. Asynchronous Performance

A methodology to comprehensively evaluate consensus protocol performance under asynchronous network conditions remains an open research problem [55]. The only published method for asynchronous evaluation appears in [25], which we follow in this paper.

This experiment evaluates RACS and SADL-RACS under simulated network attack scenarios. The attacker increases the egress packet latency of a randomly selected minority of replicas by 500ms in dynamic time epochs. The experiment runs in a WAN setting with 5 replicas and 5 clients. We measured throughput, latency, downtime, and time-to-recover, but due to space limits and to align with recent literature [25], [39], we report only throughput and latency. We depict the results in Figure 6.

RACS vs {Multi-Paxos and Raft}: We observe that RACS provides 28k cmd/sec saturation throughput, in contrast, Multi-Paxos and Raft have saturation throughput at 2.8k cmd/sec. Under adversarial network conditions Multi-Paxos and Raft undergo repeated view changes, and fail at successfully committing commands. In contrast, due to the fallback mode of execution, RACS provides liveness under adversarial network conditions. Hence we prove the claim **C1**.

RACS vs SADL-RACS: We observe that SADL-RACS delivers 196k saturation throughput, thus providing 168k cmd/sec more throughput than RACS. Because SADL-RACS eliminates the leader bottleneck and the SADL protocol is robust against adversarial network conditions (as it does not rely on timeouts), SADL-RACS achieves higher throughput than RACS, even under adversarial network conditions.

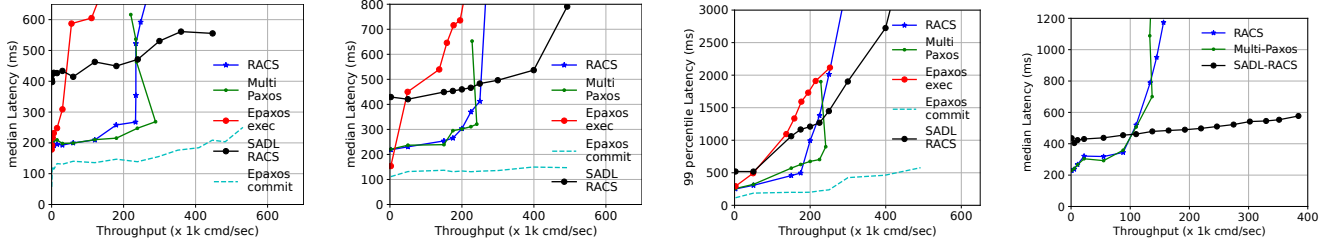


Fig. 7: Throughput versus latency for WAN normal-case execution for 3–11 number of replicas.

B. RACS WAN Normal Case Performance

In this experiment, we evaluate the normal-case synchronous performance of RACS deployed in 5 geographically distant AWS regions. Because we observed the same throughput and latency for Raft and Multi-Paxos (due to their identical structure during normal-case replication), we only depict the Multi-Paxos performance for clarity in the figures. Fig. 7b and Fig. 7c depict the experimental results using 5 replicas and 5 clients.

RACS vs Multi-Paxos: We observe in Fig. 7b that RACS delivers a saturation throughput of 200k cmd/sec throughput under 300ms median latency, which is comparable to the performance of Multi-Paxos (200k cmd/sec under 300ms latency). In the synchronous execution both RACS and Multi-Paxos have 1 round trip latency per batch of commands, hence share the same performance characteristics. Hence the experimental claim **C2** holds.

RACS vs Epaxos-commit: We observe in Fig. 7b that EPaxos-commit (without command execution) delivers a throughput of 500k+ cmd/sec under 170ms median latency. The EPaxos-commit experiment employs a conflict rate of 2% [56] hence 98% of the time, commands are committed in one round trip, without serializing through a leader replica. In contrast, RACS builds a total order of commands, serialized using a leader-replica, hence naturally the RACS performance is bottlenecked by the leader replica’s capacity.

RACS vs Epaxos-exec: As shown in Fig. 7b, the median latency of EPaxos-exec (with command execution) is 300ms higher on average than RACS in the 50k–200k cmd/sec throughput range. This higher latency stems from EPaxos’s dependency management cost [56], [57]. Hence, we conclude that when measured for execution latency, RACS outperforms EPaxos.

EPaxos is suited for applications that require only a partial order, such as key-value stores where per-key ordering is sufficient. In contrast, RACS is designed for applications that need a total order of all commands.

RACS vs SADL-RACS: As shown in Fig. 7b, SADL-RACS achieves a throughput of 500k cmd/sec, exceeding RACS by 300k cmd/sec, however, with an additional latency cost of 500ms. These results demonstrate the effectiveness of SADL in eliminating the leader bottleneck in RACS for class 2 applications that require high throughput but can tolerate moderately high latency, supporting the claim **C3**.

C. Scalability of SADL

In this experiment, we aim to quantify the scalability of SADL-RACS. We consider two factors of scalability: (1) scalability w.r.t increasing replication factor and (2) scalability w.r.t increasing payload size.

Although we conducted experiments with both Multi-Paxos and Raft, we observed the same throughput and latency behavior due to their identical protocol structure during normal-case replication (both replicate in a single network round trip, serialized through a leader). Therefore, for clarity in figures and explanation, we present only the Multi-Paxos results.

Scalability w.r.t increasing replication factor: In this experiment, we evaluate the scalability of SADL-RACS by running it with an ensemble of three (minimum replication allowed), five (common replication factor) and eleven replicas (improved robustness to concurrent replica failures), located in geographically separated AWS regions. Fig. 7 compare the scalability of SADL-RACS against pipelined RACS, pipelined Multi-Paxos, and pipelined EPaxos, for different replication factors.

RACS vs {Multi-Paxos and Raft}: We observe that the saturation throughput of Multi-Paxos and RACS decreases from 230k to 130k cmd/sec (under 600 ms median latency) when the replication factor is increased from 3–11. With increasing replica count, the leader replica in RACS and Multi-Paxos has to send and receive more messages, due to increased quorum sizes, hence the performance is bottlenecked by the leader’s bandwidth capacity.

RACS vs SADL-RACS: We observe that SADL-RACS provides a throughput of 380k cmd/sec (under 600 ms median latency), when the replication factor is 11. SADL-RACS outperforms pipelined-RACS and pipelined Multi-Paxos by 192% in the 11 replica scenario. This confirms that SADL enables RACS to increase throughput by avoiding the leader bottleneck through the decoupling of command dissemination from consensus. Hence we prove the claim **C4.1**.

Scalability w.r.t increasing payload size: In this experiment, we evaluate the impact of payload size for the SADL-RACS performance. We experiment with 3 key sizes: 8B, 64B, and 256B, used in recent SMR work [58]. Combined with 1B opcode and 8B value, these key sizes result in 17B, 73B, and 265B command sizes. We deploy SADL-RACS, pipelined Paxos and pipelined-RACS in a WAN setting with 5 replicas and 5 clients. Fig. 8 depicts the results.

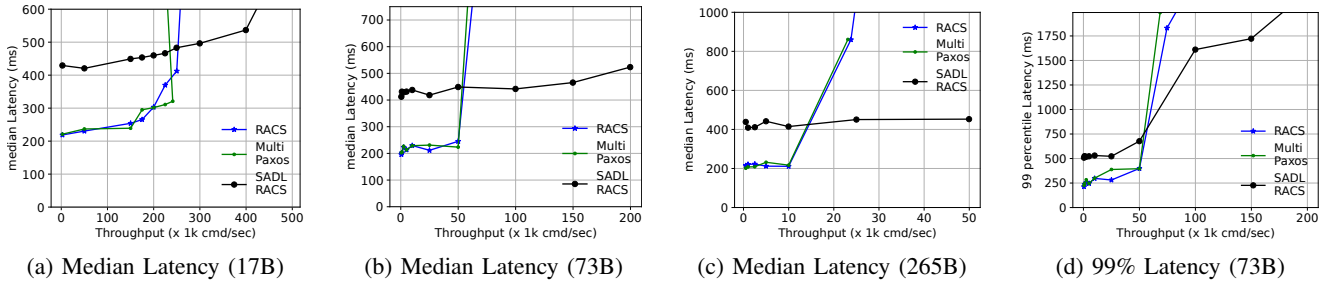


Fig. 8: Throughput versus latency for WAN normal-case execution using 17B, 73B and 265B command sizes.

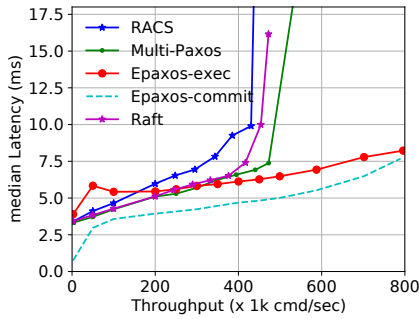


Fig. 9: Throughput versus latency for LAN normal-case.

We observe that for each command size, the saturation throughput of SADL-RACS is at least 2 times the throughput of RACS and Multi-Paxos. With increasing command size, the leader replica’s bandwidth of RACS (and Multi-Paxos) becomes the bottleneck. In contrast, thanks to the decoupling of command dissemination from consensus, SADL-RACS evenly distributes the bandwidth overhead among all the replicas, and sustains higher throughput. This proves the claim C4.2.

D. RACS LAN Normal Case Performance

In this experiment, we quantify the performance of the RACS in a LAN setting. We conduct experiments with 5 replicas and 5 clients deployed in the same AWS region. Figure 9 illustrates the LAN performance of RACS.

RACS vs {Multi-Paxos and Raft}: We observe that RACS achieves a saturation throughput of 420k cmd/sec, under a median latency upper bound of 10ms, that is comparable to the saturation throughput of Multi-Paxos (450k) and Raft (440k). Under normal case executions, RACS, Multi-Paxos, and Raft have 1 round-trip latency, serialized through a leader, hence provide comparable performance.

VII. CONCLUSION, LIMITATIONS AND FUTURE WORK

We presented RACS, the first randomized consensus protocol that simultaneously achieves three key goals; (1) robustness under adversarial network conditions, (2) performance comparable to existing leader-based protocols, under synchronous network conditions, and (3) simple design inspired by Raft, enabling seamless integration.

SADL-RACS has limitations that require future work. SADL-RACS requires at least four message hops per commit, making it less suitable for low-latency, high-throughput

applications. We propose a DAG-based redesign that merges dissemination and ordering as a plausible method to achieve both low latency and high throughput.

While SADL-RACS optimizes for performance, robustness, and simplicity, it does not address energy efficiency—its chain-based design commits blocks even at low request rates, leading to high energy use. Although energy-efficient cloud systems are well studied, consensus protocol energy use remains unexplored, opening future directions in defining energy metrics, analyzing existing protocols, and designing energy-efficient consensus protocols.

Finally, RACS assumes that a majority of replicas are connected, however, loses liveness under extreme network partitions with only one or two connected replicas. Extending RACS to support such network partitions is left for future work.

Acknowledgements.

This work was supported by (1) Myster Labs and the Sui Foundation, (2) the Austrian Science Fund (FWF) through the SFB SpyCode project F8512-N and by the WWTF through the project 10.47379/ICT22045, (3) EPFL research grants, (4) AXA Research Fund, and (5) Etherium grant.

REFERENCES

- [1] C. Cachin, R. Guerraoui, and L. Rodrigues, *Introduction to Reliable and Secure Distributed Programming*. Springer Science & Business Media, 2011.
- [2] M. Burrows, “The chubby lock service for loosely-coupled distributed systems,” in *7th Symposium on Operating Systems Design and Implementation*, 2006, pp. 335–350.
- [3] P. Hunt, M. Konar, F. P. Junqueira, and B. Reed, “[ZooKeeper]: Wait-free coordination for internet-scale systems,” in *2010 USENIX Annual Technical Conference (USENIX ATC 10)*, 2010.
- [4] J. MacCormick, N. Murphy, M. Najork, C. A. Thekkath, and L. Zhou, “Boxwood: Abstractions as the foundation for storage infrastructure.” in *Symposium on Operating Systems Design and Implementation OSDI*, vol. 4, 2004, pp. 8–8.
- [5] J. C. Corbett, J. Dean, M. Epstein, A. Fikes, C. Frost, J. J. Furman, S. Ghemawat, A. Gubarev, C. Heiser, P. Hochschild *et al.*, “Spanner: Google’s globally distributed database,” *ACM Transactions on Computer Systems (TOCS)*, vol. 31, no. 3, pp. 1–22, 2013.
- [6] J. Baker, C. Bond, J. C. Corbett, J. Furman, A. Khorlin, J. Larson, J.-M. Leon, Y. Li, A. Lloyd, and V. Yushprakh, “Megastore: Providing scalable, highly available storage for interactive services.” in *Conference on Innovative Data system Research*, 2011, pp. 223–234.
- [7] C. Xie, C. Su, M. Kapritsos, Y. Wang, N. Yaghmazadeh, L. Alvisi, and P. Mahajan, “Salt: Combining {ACID} and {BASE} in a distributed database,” in *11th USENIX Symposium on Operating Systems Design and Implementation (OSDI 14)*, 2014, pp. 495–509.

[8] D. Quintero, M. Barzaghi, R. Brewster, W. H. Kim, S. Normann, P. Queiroz, R. Simon, A. Vlad *et al.*, *Implementing the IBM General Parallel File System (GPFS) in a Cross Platform Environment*. IBM Redbooks, 2011.

[9] A. J. Mashtizadeh, A. Bittau, Y. F. Huang, and D. Mazieres, “Replication, history, and grafting in the ori file system,” in *Proceedings of the Twenty-Fourth ACM Symposium on Operating Systems Principles*, 2013, pp. 151–166.

[10] A. Grimshaw, M. Morgan, and A. Kalyanaraman, “Gffs—the xsede global federated file system,” *Parallel Processing Letters*, vol. 23, no. 02, p. 1340005, 2013.

[11] N. Bronson, Z. Amsden, G. Cabrera, P. Chakka, P. Dimov, H. Ding, J. Ferris, A. Giardullo, S. Kulkarni, H. Li, M. Marchukov, D. Petrov, L. Puzar, Y. J. Song, and V. Venkataramani, “TAO: Facebook’s distributed data store for the social graph,” in *USENIX Annual Technical Conference USENIX ATC 13*, June 2013, pp. 49–60.

[12] W. Lloyd, M. J. Freedman, M. Kaminsky, and D. G. Andersen, “Don’t settle for eventual: Scalable causal consistency for wide-area storage with cops,” in *Proceedings of the Twenty-Third ACM Symposium on Operating Systems Principles*, 2011, pp. 401–416.

[13] L. Lamport, “Paxos made simple,” *ACM SIGACT News (Distributed Computing Column)* 32, 4, vol. 32, pp. 51–58, December 2001.

[14] D. Ongaro and J. Ousterhout, “In search of an understandable consensus algorithm,” in *2014 USENIX Annual Technical Conference ATC14*, June 2014, pp. 305–319.

[15] S. Nastic, A. Morichetta, T. Puszta, S. Dusdar, X. Ding, D. Vij, and Y. Xiong, “Sloc: Service level objectives for next generation cloud computing,” *IEEE Internet Computing*, vol. 24, no. 3, pp. 39–50, 2020.

[16] J. Ding, R. Cao, I. Saravanan, N. Morris, and C. Stewart, “Characterizing service level objectives for cloud services: Realities and myths,” in *2019 IEEE International Conference on Autonomic Computing (ICAC)*. IEEE, 2019, pp. 200–206.

[17] T. Lianza and C. Snook, “Cloudflare outage,” <https://blog.cloudflare.com/a-byzantine-failure-in-the-real-world/>, November 2020.

[18] J. Moura and D. Hutchison, “Review and analysis of networking challenges in cloud computing,” *Journal of Network and Computer Applications*, vol. 60, pp. 113–129, 2016.

[19] D. De Sensi, T. De Matteis, K. Taranov, S. Di Girolamo, T. Rahn, and T. Hoefer, “Noise in the clouds: Influence of network performance variability on application scalability,” *Proceedings of the ACM on Measurement and Analysis of Computing Systems*, vol. 6, no. 3, pp. 1–27, 2022.

[20] I. Moraru, D. G. Andersen, and M. Kaminsky, “There is more consensus in egalitarian parliaments,” in *Proceedings of the Twenty-Fourth ACM Symposium on Operating Systems Principles*, November 2013, pp. 358–372.

[21] Y. Mao, F. Junqueira, and K. Marzullo, “Mencius: Building efficient replicated state machines for WANs,” in *8th USENIX Symposium on Operating Systems Design and Implementation (OSDI 08)*, December 2008.

[22] A. Charapko, A. Ailijiang, and M. Demirbas, “PigPaxos: Devouring the communication bottlenecks in distributed consensus,” in *Proceedings of the 2021 International Conference on Management of Data*, June 2021, pp. 235–247.

[23] L. Lamport, “Generalized consensus and Paxos,” *Microsoft Research Technical Report MSR-TR-2005-33*, p. 60, 2005. [Online]. Available: <https://www.microsoft.com/en-us/research/publication/generalized-consensus-and-paxos/>

[24] P. Tennage, C. Basescu, E. K. Kogias, E. Syta, P. Jovanovic, and B. Ford, “Baxos: Backing off for robust and efficient consensus,” *arXiv preprint arXiv:2204.10934*, December 2024.

[25] P. Tennage, C. Basescu, L. Kokoris-Kogias, E. Syta, P. Jovanovic, V. Estrada, and B. Ford, “QuePaxa: Escaping the tyranny of timeouts in consensus,” *Proceedings of the 29th Symposium on Operating Systems Principles (SOSP)*, Oct. 2023.

[26] M. Ben-Or, “Another advantage of free choice (extended abstract) completely asynchronous agreement protocols,” in *Proceedings of the Second Annual ACM symposium on Principles of Distributed Computing*, August 1983, pp. 27–30.

[27] B. Wang, S. Liu, H. Dong, X. Wang, W. Xu, J. Zhang, P. Zhong, and Y. Zhang, “Bandle: Asynchronous state machine replication made efficient,” in *Proceedings of the Nineteenth European Conference on Computer Systems*, ser. EuroSys ’24. New York, NY, USA: Association for Computing Machinery, 2024, p. 265–280. [Online]. Available: <https://doi.org/10.1145/3627703.3650091>

[28] G. Danezis, L. Kokoris-Kogias, A. Sonnino, and A. Spiegelman, “Narwhal and Tusk: A DAG-based Mempool and efficient BFT consensus,” in *Proceedings of the Seventeenth European Conference on Computer Systems (EuroSys ’22)*, Mar. 2022, pp. 34–50.

[29] J. Meyerson, “The Go programming language,” *IEEE Software*, vol. 31, no. 5, pp. 104–104, 2014.

[30] “Transmission control protocol,” Sep. 1981, rFC 793.

[31] J. Aspnes, “Randomized protocols for asynchronous consensus,” *Distributed Computing*, vol. 16, no. 2–3, pp. 165–175, 2003.

[32] E. Rescorla and T. Dierks, “The transport layer security (TLS) protocol version 1.3,” August 2018, rFC 8446.

[33] M. J. Fischer, N. A. Lynch, and M. S. Paterson, “Impossibility of distributed consensus with one faulty process,” *Journal of the ACM (JACM)*, vol. 32, no. 2, pp. 374–382, 1985.

[34] B. M. Oki and B. H. Liskov, “Viewstamped replication: A new primary copy method to support highly-available distributed systems,” in *Proceedings of the Seventh Annual ACM Symposium on Principles of Distributed Computing*, january 1988, pp. 8–17.

[35] P. J. Marandi, M. Primi, N. Schiper, and F. Pedone, “Ring Paxos: A high-throughput atomic broadcast protocol,” in *IEEE/IFIP International Conference on Dependable Systems & Networks (DSN)*. IEEE, June 2010, pp. 527–536.

[36] H. Ng, S. Haridi, and P. Carbone, “Omni-Paxos: Breaking the barriers of partial connectivity,” in *Eighteenth European Conference on Computer Systems (EuroSys)*, May 2023, pp. 314–330.

[37] A. Ailijiang, A. Charapko, M. Demirbas, and T. Kosar, “WPaxos: Wide area network flexible consensus,” *IEEE Transactions on Parallel and Distributed Systems*, vol. 31, no. 1, pp. 211–223, 2019.

[38] H. Pan, J. Tuglu, N. Zhou, T. Wang, Y. Shen, X. Zheng, J. Tassarotti, L. Tseng, and R. Palmieri, “Rabia: Simplifying state-machine replication through randomization,” in *Proceedings of the ACM SIGOPS 28th Symposium on Operating Systems Principles*, October 2021, pp. 472–487.

[39] P. Jovanovic, L. Kokoris-kogias, B. Kumara, A. Sonnino, P. Tennage, and I. Zablotchi, “Mahi-mahi: Low-latency asynchronous bft dag-based consensus,” in *IEEE ICDCS 2025, 45th IEEE International Conference on Distributed Computing Systems*, 2025.

[40] I. Keidar, E. Kokoris-Kogias, O. Naor, and A. Spiegelman, “All you need is dag,” in *Proceedings of the 2021 ACM Symposium on Principles of Distributed Computing*, 2021, pp. 165–175.

[41] M. Kogias and E. Bugnion, “HovercRaft: Achieving scalability and fault-tolerance for microsecond-scale datacenter services,” in *Proceedings of the Fifteenth European Conference on Computer Systems*, April 2020, pp. 1–17.

[42] HashiCorp, “Raft: Golang implementation of the raft consensus protocol,” <https://github.com/hashicorp/raft>, 2013, accessed: 2025-01-12.

[43] P. Tennage, “Paxos and Raft,” Sep. 2023, GitHub repository <https://github.com/dedis/paxos-and-raft>.

[44] F. Li, D. Yu, H. Yang, J. Yu, H. Karl, and X. Cheng, “Multi-armed-bandit-based spectrum scheduling algorithms in wireless networks: A survey,” *IEEE Wireless Communications*, vol. 27, no. 1, pp. 24–30, 2020.

[45] The etcd Authors, “etcd: Distributed reliable key-value store,” <https://etcd.io/>, 2013, accessed: 2024-01-14.

[46] J. Kreps, N. Narkhede, J. Rao *et al.*, “Kafka: A distributed messaging system for log processing,” in *Proceedings of the NetDB*, vol. 11, no. 2011. Athens, Greece, 2011, pp. 1–7.

[47] Apache Software Foundation, “Apache hadoop: Open-source framework for distributed storage and processing of large data sets,” <https://hadoop.apache.org/>, 2006, accessed: 2024-01-14.

[48] A. Spiegelman, N. Giridharan, A. Sonnino, and L. Kokoris-Kogias, “Bullshark: Dag bft protocols made practical,” in *Proceedings of the 2022 ACM SIGSAC Conference on Computer and Communications Security*, 2022, pp. 2705–2718.

[49] Google, “Protocol buffers,” <https://developers.google.com/protocol-buffers/>, 2020.

[50] I. Moraru, D. G. Andersen, M. Kaminsky, and P. Tennage, “EPaxos go-lang,” <https://github.com/dedis/quepaxa-ePaxos-open-loop>, Sep. 2023.

[51] Amazon, “AWS instance types,” <https://aws.amazon.com/ec2/instance-types/>, 2023.

[52] Ubuntu, “Ubuntu Linux,” <https://releases.ubuntu.com/focal/>, 2023.

[53] V. Mihailenco, Denissenko, and Dimitrij, “Go lang Redis,” <https://github.com/redis/go-redis>, 2023.

- [54] B. Schroeder, A. Wierman, and M. Harchol-Balter, “Open versus closed: A cautionary tale,” in *Proceedings of the 3rd USENIX Symposium on Networked Systems Design and Implementation (NSDI 06)*. USENIX, May 2006.
- [55] P. Tennage, S. Mishra, A. Sonnino, L. K. Kogias, P. Jovanovic, and B. Ford, “Consenstress: A framework to torture test consensus protocols,” in *EuroSys 2025 (poster)*, 2025.
- [56] S. Tollman, S. J. Park, and J. K. Ousterhout, “EPaxos revisited,” in *USENIX Symposium on Networked Systems Design and Implementation (NSDI 21)*, April 2021, pp. 613–632.
- [57] V. S. Matte, A. Charapko, and A. Aghayev, “Scalable but wasteful: Current state of replication in the cloud,” in *Proceedings of the 13th ACM Workshop on Hot Topics in Storage and File Systems*, July 2021, pp. 42–49.
- [58] M. Alimadadi, H. Mai, S. Cho, M. Ferdman, P. Milder, and S. Mu, “Waverunner: An elegant approach to hardware acceleration of state machine replication,” in *20th USENIX Symposium on Networked Systems Design and Implementation (NSDI 23)*, 2023, pp. 357–374.

APPENDIX

A. Definition

elected-fallback block: We refer to an fallback block B_f generated in view v with level 2 as an elected-fallback block, if the common-coin-flip(v) returns the index of the proposer p_l who generated B_f in the view v and if the \langle asynchronous-complete \rangle for B_f exists in the first $n - f$ \langle asynchronous-complete \rangle messages received.

B. Proof of agreement

Theorem 1. *Let B and \tilde{B} be two blocks with rank (v, r) . Each of B and \tilde{B} can be of type: (1) synchronous block which collects at least $n - f$ votes or (2) elected-fallback block or (3) level 1 fallback block which is a parent of an elected-fallback block. Then \tilde{B} and B are the same.*

Proof. This holds directly from the block formation – if both B and \tilde{B} has the same rank, then due to quorum intersection, there exists at least one node who voted for both blocks in the same rank, which is a contradiction to our assumption of non malicious nodes. \square

Theorem 2. *Let B and \tilde{B} be two adjacent blocks, then $\tilde{B}.r = B.r + 1$ and $\tilde{B}.v \geq B.v$.*

Proof. According to the algorithm, there are three instances where a new block is created.

- Case 1: when $isAsync = \text{false}$ and L_{vcur} creates a new synchronous block by extending the $block_{high}$ with rank (v, r) . In this case, L_{vcur} creates a new block with round $r + 1$. Hence the adjacent blocks have monotonically increasing round numbers.
- Case 2: when $isAsync = \text{true}$ and upon collecting $n - f$ \langle timeout \rangle messages in view v . In this case, the replica selects the $block_{high}$ with the highest rank (v, r) , and extends it by proposing a level 1 fallback block with round $r + 1$. Hence the adjacent blocks have monotonically increasing round numbers.
- Case 3: when $isAsync = \text{true}$ and upon collecting $n - f$ \langle vote-async \rangle messages for a level 1 fallback block. In this case, the replica extends the level 1 block by proposing a level 2 block with round $r + 1$. Hence the adjacent blocks have monotonically increasing round numbers.

The view numbers are non decreasing according to the algorithm. Hence Theorem 2 holds. \square

Theorem 3. *If a synchronous block B_c with rank (v, r) is committed, then all future blocks in view v will extend B_c .*

Proof. We prove this by contradiction.

Assume there is a committed block B_c with $B_c.r = r_c$ (hence all the blocks in the path from the genesis block to B_c are committed). Let block B_s with $B_s.r = r_s$ be the round r_s block such that B_s conflicts with B_c (B_s does not extend B_c). Without loss of generality, assume that $r_c < r_s$.

Let block B_f with $B_f.r = r_f$ be the first valid block formed in a round r_f such that $r_s \geq r_f > r_c$ and B_f is the first block

from the path from genesis block to B_s that conflicts with B_c ; for instance B_f could be B_s . L_{vcur} forms B_f by extending its $block_{high}$. Due to the minimality of B_f (B_f is the first block that conflicts with B_c), $block_{high}$ contain either B_c or a block that extends B_c . Since $block_{high}$ extends B_c , B_f extends B_c , thus we reach a contradiction. Hence no such B_f exists. Hence all the blocks created after B_c in the view v extend B_c . \square

Theorem 4. *If a synchronous block B with rank (v, r) is committed, an elected-fallback block \tilde{B} of the same view v will extend that block.*

Proof. We prove this by contradiction. Assume that a synchronous block B is committed in view v and an elected-fallback block \tilde{B} does not extend B . Then, the parent level 1 block of \tilde{B} , \tilde{B}_p , also does not extend B .

To form the level 1 \tilde{B}_p , the replica collects $n-f$ $\langle \text{timeout} \rangle$ messages, each of them containing the $block_{high}$. If B is committed, by theorem 3, at least $n-f$ replicas should have set (and possibly sent) B or a block extending B as the $block_{high}$. Hence by intersection of the quorums \tilde{B}_p extends B , thus we reach a contradiction. \square

Theorem 5. *At most one level 2 fallback block from one proposer can be committed in a given view change.*

Proof. Assume by way of contradiction that 2 level 2 fallback blocks from two different proposers are committed in the same view. A level 2 fallback block B is committed in the fallback phase if the common-coin-flip(v) returns the proposer of B as the elected proposer. Since the common-coin-flip(v) outputs the same elected proposer across different replicas, this is a contradiction. Thus all level 2 fallback blocks committed during the same view are from the same proposer.

Assume now that the same proposer proposed two different level 2 fallback blocks. Since no replica can equivocate, this is absurd.

Thus at most one level 2 fallback block from one proposer can be committed in a given view change. \square

Theorem 6. *Let B be a level 2 elected-fallback block that is committed, then all blocks proposed in the subsequent rounds extend B .*

Proof. We prove this by contradiction. Assume that level two elected-fallback block B is committed with rank (v, r) and block \tilde{B} with rank (\tilde{v}, \tilde{r}) such that $(\tilde{v}, \tilde{r}) > (v, r)$ is the first block in the chain starting from B that does not extend B . \tilde{B} can be formed in two occurrences: (1) \tilde{B} is a synchronous block in the view $v+1$ or (2) \tilde{B} is a level 1 fallback block with a view strictly greater than v . (we do not consider the case where \tilde{B} is a level 2 elected-fallback block, because this directly follows from 1)

If B is committed, then from the algorithm construction it is clear that a majority of the replicas will set B as $block_{high}$. This is because, to send a $\langle \text{asynchronous-complete} \rangle$ message with B , a replica should collect at least $n-f$ $\langle \text{vote-async} \rangle$ messages. Hence, its guaranteed that if \tilde{B} is formed in view

$v+1$ as a synchronous block, then it will observe B as the $block_{high}$, thus we reach a contradiction.

In the second case, if \tilde{B} is formed in a subsequent view, then it is guaranteed that the level 1 block will extend B by gathering from the $\langle \text{timeout} \rangle$ messages B as $block_{high}$ or a block extending B as the $block_{high}$, hence we reach a contradiction. \square

Theorem 7. *There exists a single history of committed blocks.*

Proof. Assume by way of contradiction there are two different histories H_1 and H_2 of committed blocks. Then there is at least one block from H_1 that does not extend at least one block from H_2 . This is a contradiction with theorems 3, 4 and 6. Hence there exists a single chain of committed blocks. \square

Theorem 8. *For each committed replicated log position r , all replicas contain the same block.*

Proof. By theorem 2, the committed chain will have incrementally increasing round numbers. Hence for each round number (log position), there is a single committed entry, and by theorem 1, this entry is unique. This completes the proof. \square

C. Proof of termination

Theorem 9. *If at least $n-f$ replicas enter the fallback phase of view v by setting isAsync to true, then eventually they all exit the fallback phase and set isAsync to false.*

Proof. If $n-f$ replicas enter the fallback path, then eventually all replicas (except for failed replicas) will enter the fallback path as there are less than $n-f$ replicas left on the synchronous path due to quorum intersection, so no progress can be made on the synchronous path and all replicas will timeout. As a result, at least $n-f$ correct replicas will broadcast their $\langle \text{timeout} \rangle$ message and all replicas will enter the fallback path.

Upon entering the fallback path, each replica creates a fallback block with level 1 and broadcasts it. Since we use perfect point-to-point links, eventually all the level 1 blocks sent by the $n-f$ correct replicas will be received by each replica in the fallback path. At least $n-f$ correct replicas will send them $\langle \text{vote-async} \rangle$ messages if the rank of the level 1 block is greater than the rank of the replica. To ensure liveness for the replicas that have a lower rank, the algorithm allows catching up, so that nodes will adopt whichever level 1 block which received $n-f$ $\langle \text{vote-async} \rangle$ arrives first. Upon receiving the first level 1 block with $n-f$ $\langle \text{vote-async} \rangle$ messages, each replica will send a level 2 fallback block, which will be eventually received by all the replicas in the fallback path. Since the level 2 block proposed by any block passes the rank test for receiving a $\langle \text{vote-async} \rangle$, eventually at least $n-f$ level 2 blocks get $n-f$ $\langle \text{vote-async} \rangle$. Hence, eventually at least $n-f$ replicas send the $\langle \text{asynchronous-complete} \rangle$ message, and exit the fallback path. \square

Theorem 10. *With probability $p > \frac{1}{2}$, at least one replica commits an elected-fallback block after exiting the fallback path.*

Proof. Let leader $L_{elected}$ be the output of the common-coin-flip(v). A replica commits a block during the fallback mode if the \langle asynchronous-complete \rangle message from $L_{elected}$ is among the first $n - f$ \langle asynchronous-complete \rangle messages received during the fallback mode, which happens with probability at least greater than $\frac{1}{2}$. Hence with probability no less than $\frac{1}{2}$, each replica commits a chain in a given fallback phase. \square

Theorem 11. *A majority of replicas keep committing new blocks with high probability.*

Proof. We first prove this theorem for the basic case where all replicas start the protocol with $v = 0$. If at least $n - f$ replicas eventually enter the fallback path, by theorem 9, they eventually all exit the fallback path, and a new block is committed by at least one replica with probability no less than $\frac{1}{2}$. According to the asynchronous-complete step, all nodes who enter the fallback path enter view $v = 1$ after exiting the fallback path. If at least $n - f$ replicas never set *isAsync* to true, this implies that the sequence of blocks produced in view 1 is infinite. By Theorem 2, the blocks have consecutive round numbers, and thus a majority replicas keep committing new blocks.

Now assume the theorem 11 is true for view $v = 0, \dots, k-1$. Consider the case where at least $n - f$ replicas enter the view $v = k$. By the same argument for the $v = 0$ base case, $n - f$ replicas either all enter the fallback path commits a new block with $\frac{1}{2}$ probability, or keeps committing new blocks in view k . Therefore, by induction, a majority replicas keep committing new blocks with high probability. \square

Theorem 12. *Each client command is eventually committed.*

Proof. If each replica repeatedly keeps proposing the client commands until they become committed, then eventually each client command gets committed according to theorem 11. \square